Proliferation of cosine-tuning in both artificial spiking and cortical neural networks during learning

Tengjun Liu[1,2] **Yansong Chua**[3*] **Yiwei Zhang**[1,2] **Yuxiao Ning**[1,2]

Guihua Wan[1] **Zijun Wan**[1,2] **Shaomin Zhang**[1,2,4,5*]

Weidong Chen[1,6]

[1] Key Laboratory of Biomedical Engineering of Ministry of Education, Qiushi Academy for Advanced Studies, Zhejiang University, Hangzhou, China
[2] Department of Biomedical Engineering, Zhejiang University, Hangzhou, China
[3] China Nanhu Academy of Electronics and Information Technology (CNAEIT), Jiaxing, China
[4] State Key Laboratory of Brain-Machine Intelligence, Zhejiang University, Hangzhou, China
[5] the MOE Frontier Science Center for Brain Science & Brain-machine Integration, Zhejiang University, Hangzhou, China
[6] Department of Computer Science and Technology, Zhejiang University, Hangzhou, China
{tengjunliu,zhangevey,ningyuxiao,0916405,11715005,chenwd}@zju.edu.cn
[*]Corresponding authors: shaomin@zju.edu.cn, caiyansong@cnaeit.com

Abstract

Goal-driven deep learning (DL)-based artificial neural networks (ANNs) have shown many promising bio-functional similarities with different biological neural systems, though they are less reported to model the motor neural system. Even less is known about whether goal-driven DL-based spiking neural networks (SNNs) exhibit similar bio-functional properties or predictive capabilities in the motor system. In this study, we employed the motorSRNN, a recurrent SNN inspired by the primate neural motor circuit. It successfully decoded cortical spike trains (CSTs) from the primary motor cortex (M1) of two monkeys performing a reaching task. Notably, the motorSRNN replicated bio-functional properties at population and circuit levels, closely matching those observed in biology. Moreover, motorSRNN captured and cultivated more significantly cosine-tuned neurons (SCtNs) and maintained stable proliferation existence during learning, suggesting that similar processes may occur in a learning biological neural network. To test this prediction, we designed a brain-machine interface (BMI) experiment in which the cortical neural networks in M1 of two monkeys learned to modulate their activities to control a new decoder in four widely spaced sessions. Our results confirmed that new task learning indeed induced the stable existence of proliferation of SCtNs in M1. In summary, the goal-driven motorSRNN demonstrates bio-functional similarity and predictive capability, offering a framework for motor circuit modeling.

1 Introduction

Understanding the neural basis of perception and motor functions has long been a central focus in neuroscience. Goal-driven DL-based ANNs have successfully elucidated perceptual neural information processing across various systems [1], including the visual cortex [2–5], Whisker-Trigeminal

1^{st} Workshop on NeuroAI @ 38th Conference on Neural Information Processing Systems (NeurIPS 2024).

system [6], prefrontal cortex [7, 8], and brain areas involved in natural language processing [9]. For instance, convolutional neural networks (CNNs) trained for object classification show object and face separation similar to the biological brain [2] , while recurrent neural networks (RNNs) trained on cognitive tasks replicate prefrontal cortex changes from adolescence to adulthood [8]. However, when it comes to motor neural circuits, the resemblance between ANNs and biological systems remains less explored. David et al. showed that RNNs trained for motor activity generation in simulations exhibit dynamics comparable to those of motor cortex neurons in non-human primates [10]. Additionally, a modular RNN trained to generate object-specific grasping activities captured neural dynamics in the visuomotor circuit of monkeys [11].

Spurred by such insights, researchers have increasingly adopted DL-based ANNs directly as models to better understand biological neural mechanisms. Notably, Pouya et al. developed a DL-based CNN image synthesis method that predicted neuronal tuning in the primate V4 area and controlled neural activities accordingly [12]. Furthermore, deep CNNs have also been used to construct a low-dimensional space for object representation, the existence of which was validated within the biological inferotemporal (IT) cortex [13].

SNNs, known for their biological realism through spike-based communication, are emerging as more authentic neural models [14]. They have been used to study various neural functions such as proactive inhibitory control [15], real-time vision [16], sound source localization [17], cerebellar pathologies [18], and sleep [19]. Recently, DL-based SNNs have also been trained for various goal-driven tasks, such as decoding MNIST [20], CIFAR [21], Heidelberg Spiking Dataset (SHD) [22], and cortical spike trains (CST) from the biological motor cortex [23–26], with promising results. However, it's unclear if these goal-driven DL-based SNNs can replicate the bio-functional similarities like ANNs and serve effectively as models for neural mechanism studies. While Chen et al. demonstrated that a large-scale SNN of the primary visual cortex shares neural coding properties with the brain [27], whether bio-functional similarities of neural motor circuits exist in these SNNs are yet to be clarified. Therefore, our study aims to assess the bio-functional similarities of goal-driven DL-based SNNs.

Beyond identifying bio-functional similarities, establishing predictive validity of neural mechanisms is essential to demonstrate the utility of any neural model. BMIs are widely used to probe neural mechanisms, especially in motor learning [28–32]. For example, Hennig et al. showed that abrupt changes in motor cortex population activity, reflecting internal state fluctuations, systematically influence the learning of new BMI mappings [31]. Likewise, Losey et al. found that learning a new BMI mapping can alter neural activity for familiar tasks, leaving a 'memory trace' but without affecting performance [30]. In this study, after examining bio-functional similarities, we assess the predictive capacity of goal-driven DL-based SNNs for neural mechanisms in motor learning, leveraging BMIs' advantages.

This research employs the motorSRNN, inspired by the primate neural motor circuit, to decode CSTs from monkeys into the directions of their moving hands. We first assessed the bio-functional similarity between the motorSRNN and the primate motor circuit, then examined learning-induced changes in the tuning properties of motorRSNN's artificial neurons. Finally, anticipating similar changes during biological learning, we propose to validate these findings using a BMI approach.

2 Methods

Dataset A joystick control experiment involved two monkeys (B04 and C05) performing a 4-direction center-out reaching task. Neural and joystick signals were recorded concurrently. The neural signals are then filtered, detected, and sorted to extract spike trains. These CSTs are then segmented into samples and used to classify joystick moving directions (*Top*, *bottom*, *left*, and *right*). One-tenth of the samples were randomly selected for the validation set, with the rest used for the training set. For more details, see Sections 1.1.1 and 1.2.1 in the supplementary material (SM).

motorSRNN motorSRNN is a recurrent SNN inspired by the motor circuit in primates, as shown in FIg. S2. It features a multi-layer structure with adaptive leaky integrate-and-fire (ALIF) neurons in layers simulating the motor cortex (MC), subcortical region (SC), and spine (Sp), and non-firing leaky integrator (LI) neurons in the layer representing muscles (Ms). recurrent SNNs are embedded in layer MC1, MC2, and SC, while a feedforward SNN is used in layer Sp. Layer Ms outputs cumulative probabilities for 4 labels over time, with the highest cumulative probability at the final moment

indicating the predicted label. Membrane time constant (TC) τ_m and the adaptive threshold TC τ_{adp} of motorSRNN are trainable. Surrogate gradient descent and back-propagation-through-time are used for model training. For further details, see Section 1.3 in the SM.

BMI setting In the BMI mind control experiment, monkeys C05 and B11 were trained to modulate activities in their cortical neural networks in M1 to control a cursor in a 4-radial center-out task using a Kalman filter (Fig. 3A). Neural signals were processed through filtering, spike detection, and sorting, with training divided into look, assisted, and pure mind control blocks. The look and pure mind control blocks corresponded to the before-training and after-training phases, while the assisted and pure mind control blocks together represented the during-training phase. Sessions were widely spaced to ensure neural variability and achieving more generalizable results. For more details, see Section 1.1.2 and 1.2.2 in the SM. All animal experiments above were conducted with approval from the Experimental Animal Welfare Ethics Committee of Zhejiang University.

3 Results

Designed to establish a connection between the brain and the externals, motorSRNN achieved average accuracies on held-out data of 89.4%±0.4% on B04 and 79.9%±0.5% on C05 for four-direction classification tasks [26]. We then investigate how it learns the task and its potential for exhibiting bio-functional similarities.

3.1 Proliferation and persistency of cosine-tuning in motorSRNN

Previous studies have identified cosine-tuned pyramidal neurons in the motor cortex that exhibit a preferred direction (PD) to the primate's hand movement direction [33]. This discovery has been fundamental to numerous motor BMI applications [34–37]. Cosine-tuning is a key characteristic of the recorded biological neurons producing the input CSTs. Some artificial SCtNs in the motorSRNN of the movement direction labels were found even before learning, interestingly with more appearing after learning, particularly in layer MC1, as illustrated in Fig. 1A-D. More example SCtNs are shown in Fig. S3. The relatively small number of SCtNs in motorSRNN before training reflected the cosine-tuning purely induced by the input CSTs collected from M1.

For both dataset B04 and C05, Fig. 1C-D showed the distribution of R^2 values from cosine fits of the neuronal firing rates in layer MC1 of motorSRNN. After training, most neurons achieved high R^2, with many showing significant improvement. To avoid overestimating the dependence between firing rates and reaching directions, a statistical F-test was applied, considering R^2 only if $p < 0.05$ in the fitting. Neurons with significant cosine tuning and $R^2 > 0.7$ are referred to as SCtNs. Fig. 1B compared the number of SCtNs in layer MC1 before and after training, showing a marked increase post-training, indicating that motorSRNN effectively captured and proliferated more SCtNs.

However, these results were based on the epoch with the highest validation accuracy, leaving the stability of this proliferation over epochs uncertain. To assess its persistency, we examined whether the number of SCtNs remained significantly elevated across training epochs for both datasets. Our findings confirmed that this proliferation was stable across epochs, as demonstrated in Fig. 1E-F.

3.2 Bio-functional similarity between the neural motor circuit and motorSRNN

The results above demonstrate a transfer and proliferation of cosine-tuning from the input CSTs to the motorSRNN. We next examined whether the motorSRNN developed additional bio-functional properties or simply utilized the input information.

Population level Symmetry is an important feature of neuronal PD distribution in the motor cortex of primates [38, 39, 43]. We analyzed PD distributions of SCtNs in motorSRNN's layer MC1 using datasets B04 and C05. Initially, the PD polar distribution of SCtNs in layer MC1, motorSRNN (Fig. 2B-C, yellow) resembled the innate distribution from input CSTs recorded from B04 and C05 (Fig. 2A). Post-training, the decreased RVL (see section 3.2 in SM) indicated increased symmetry in these PD distributions (Fig. 2B-C, blue), aligning with in vivo experimental observations (Fig. 2D). Note that peaks in the polar plot indicate more neurons tuned to specific directions, but not deeper tuning.

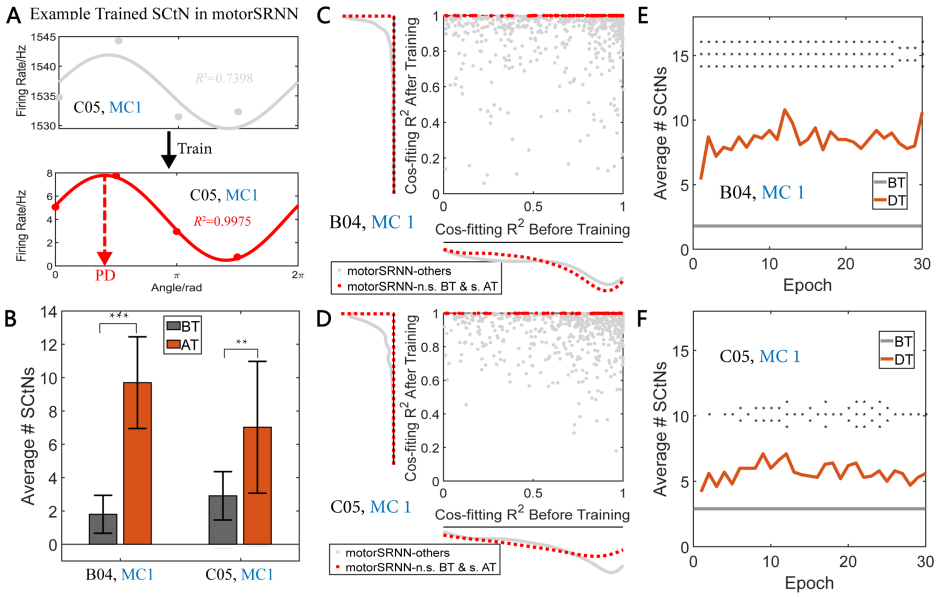

Figure 1: **Cosine-tuning was captured and proliferated in layer MC1 of motorSRNN, and existed persistently.** (A) Example SCtN in layer MC 1, motorSRNN after training. Dots represent average firing rates for different directional labels: *Left*: 0, *Up*: $\pi/2$, *Right*: π, *Down*: $3\pi/2$. Curves show fitted cosine functions, with dashed arrows indicating the PD. (B) The average number of SCtNs in layer MC 1, motorSRNN before and after training over 10 runs for dataset B04 and C05. Error bars represent standard deviation. (C-D) R^2 values of cosine fits for neurons' firing rates in layer MC1, motorSRNN for datasets B04 (C) and C05 (D), before and after training. Gray dots represent pooled neurons from 10 runs, while red dots indicate neurons that gained significant cosine tuning ($p < 0.05$) post-training, but not before ($p \geq 0.05$). Marginal density plots show data distribution. (E-F) Average number of SCtNs during training for datasets B04 (E) and C05 (F). Red curves show SCtN counts during training, while gray lines indicate counts before training. BT: before training, AT: after training, DT: during training. Under 2-sample t-test, n.s.: not significant ($p \geq 0.05$), *: $p < 0.05$, **: $p < 0.01$, ***: $p < 0.001$.

Additionally, the distributions of membrane TCs of neurons in layer MC1, motorSRNN after training (Fig. 2E) are also qualitatively similar to biological observations (Fig. 2F).

Circuit level The motorSRNN's unique M1LC, inspired by cortico-motoneuronal (CM) connections specific to primates [44], was explored through ablation experiments. Biological CM connections are key to dexterous hand and finger control [45], leading us to hypothesize that M1LC ablation would increase the standard deviation during training. The ablation results confirmed our hypothesis, showing significant increases in standard deviations (Fig. 2G), highlighting the bio-functional similarity between the M1LC topology in motorSRNN and biological CM connections.

3.3 Proliferation and persistency of cosine-tuning in the biological motor cortex

In section 3.1, we observed the proliferation and persistency of cosine-tuning in layer MC1 of motorSRNN. To explore whether similar effects occur in the motor cortex of primates (the biological counterpart of MC1) during new task learning, we conducted BMI experiments. Monkeys learnt to modulate the activities in their cortical neural networks to adapt to a new Kalman filter decoder. To generalize results, one new monkey B11 together with C05 were trained in widely separated sessions (Fig. S1). Each session began with a look block (before learning), followed by learning blocks with decreasing assistance (during learning), and ended with pure mind control blocks (after learning). Both monkeys successfully modulated neural activity to control the cursor, with success rates of 95.60% and 90.65%, respectively. We compared the number of SCtNs in the M1 neurons of C05 and B11 before and after training (Fig. 3B). Both monkeys showed significant increases in SCtNs after

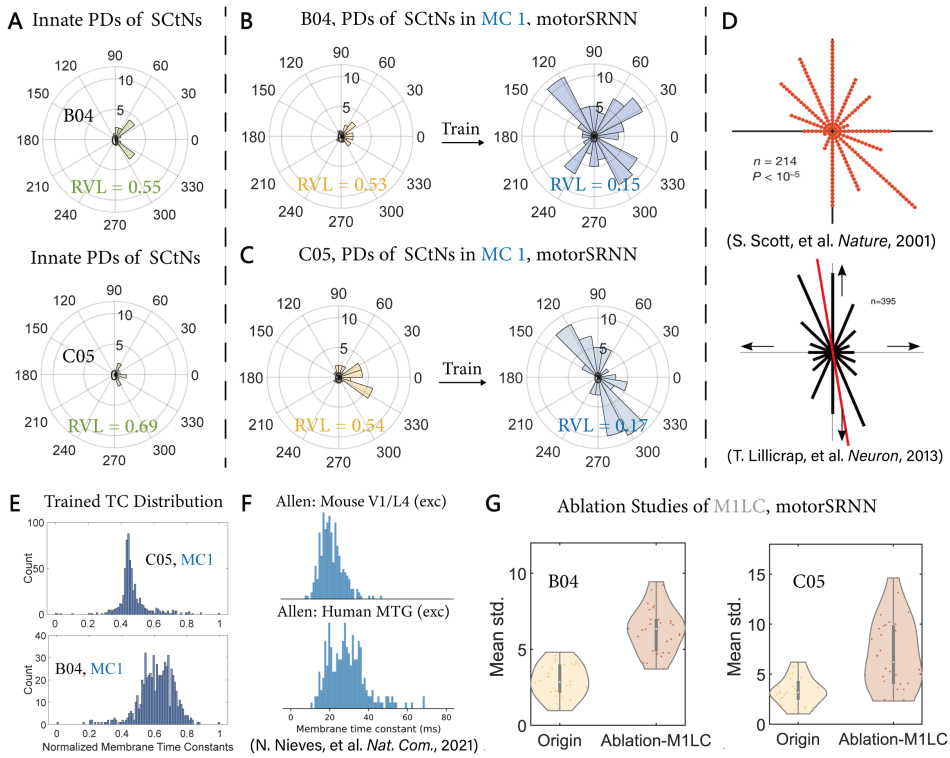

Figure 2: **Bio-functional similarities of motorSRNN at population and circuit levels.** (A) PD polar distribution of SCtNs from recorded CSTs in monkeys B04 and C05. RVL: resultant vector length. (B-C) PD polar distribution of SCtNs in motorSRNN layer MC1, before (yellow) and after (blue) training on B04 and C05. 10 runs pooled. (D) Observed PD symmetric distribution of SCtNs from large-scale recording of MC in monkeys [38, 39]. (E) Normalized membrane TC distributions of neurons in MC1, motorSRNN, after training on B04 and C05. (F) Observed TC distributions for spiny (excitatory) cells in mouse V1 layer 4 and human MTG [40–42]. 10 runs pooled. (G) Mean standard deviation of decoding performance over 10 random initialization at each epoch for original (yellow) and M1LC-ablated (blown) motorSRNNs, all epochs pooled.

learning, consistent with layer MC1 of motorSRNN (Fig. 1B). We also assessed the persistency of this proliferation during training. Results indicated a stable existence of increase in SCtNs across blocks (Fig. 3C), confirming that new task learning induces both the proliferation and persistency of cosine-tuning in the primate motor cortex. Note that here proliferation refers to a short-term increase in SCtN number, not modulation depth [46] or long-term number increase [47].

4 Discussion

Summary This study examines whether motorSRNN, a goal-driven DL-based SNN, shares bio-functional properties with the primate motor circuit and makes verifiable predictions. motorSRNN mirrors bio-functional similarities at population and circuit levels. And it predicts that proliferation and persistency of cosine-tuning occurs during new task learning in the cortical neural networks of the motor cortex in monkeys, which was further validated by BMI experiments.

Limitations & impacts While the motorSRNN shows emergent bio-functional similarities, it only simplistically mimics the primate neural motor circuit. Incorporating more biological facts [48–50] could enhance the model's biological authenticity, potentially leading to better predictions of neural computation mechanisms. This study suggests that a goal-driven DL-based SNN offers a promising framework for comprehending the brain, potentially aiding in curing neural disorders.

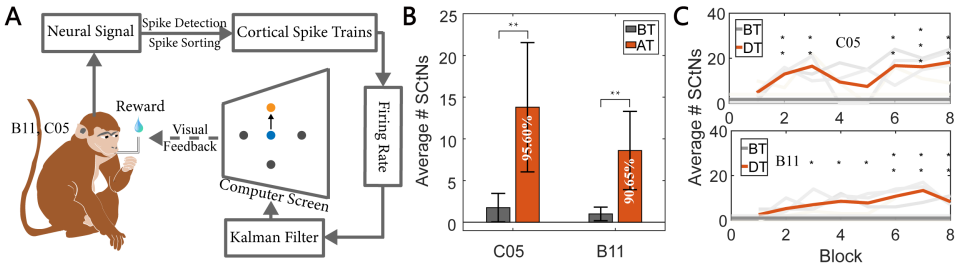

Figure 3: **BMI experimental paradigm and changes of SCtNs counts for monkey C05 and B11.** (A) BMI experimental paradigm. Two monkeys (B11 & C05) were trained to control the activities in their cortical neural networks to complete a 4-direction task. A Kalman filter mapped their neural signals to move a blue cursor toward an orange target on the screen. Successful task completion earned them a reward. (B-C) Same result presenting way as Fig. 1B, E-F. White text on the red bars shows the average success rates of pure mind control for the two monkeys.

Acknowledgments

This work is funded by: the STI 2030-Major Projects (No.2022ZD0208600), Key R&D Program for Zhejiang (No. 2021C03003, 2022R52033, 2022C03029, 2023C03081, 2023C03026, 2024C03002), and ZJU Doctoral Graduate Academic Rising Star Development Program (No. 2023059). We thank Yunying Wu, and Zihao Li for their insightful discussion and suggestions.

References

[1] Daniel LK Yamins and James J DiCarlo. Using goal-driven deep learning models to understand sensory cortex. *Nature neuroscience*, 19(3):356–365, 2016.

[2] Katharina Dobs, Julio Martinez, Alexander JE Kell, and Nancy Kanwisher. Brain-like functional specialization emerges spontaneously in deep neural networks. *Science advances*, 8(11): eabl8913, 2022.

[3] Seyed-Mahdi Khaligh-Razavi and Nikolaus Kriegeskorte. Deep supervised, but not unsupervised, models may explain it cortical representation. *PLoS computational biology*, 10(11): e1003915, 2014.

[4] Khaled Nasr and Andreas Nieder. Spontaneous representation of numerosity zero in a deep neural network for visual object recognition. *Iscience*, 24(11), 2021.

[5] Shahab Bakhtiari, Patrick Mineault, Timothy Lillicrap, Christopher Pack, and Blake Richards. The functional specialization of visual cortex emerges from training parallel pathways with self-supervised predictive learning. *Advances in Neural Information Processing Systems*, 34: 25164–25178, 2021.

[6] Chengxu Zhuang, Jonas Kubilius, Mitra J Hartmann, and Daniel L Yamins. Toward goal-driven neural network models for the rodent whisker-trigeminal system. *Advances in Neural Information Processing Systems*, 30, 2017.

[7] Khaled Nasr, Pooja Viswanathan, and Andreas Nieder. Number detectors spontaneously emerge in a deep neural network designed for visual object recognition. *Science advances*, 5(5): eaav7903, 2019.

[8] Yichen Henry Liu, Junda Zhu, Christos Constantinidis, and Xin Zhou. Emergence of prefrontal neuron maturation properties by training recurrent neural networks in cognitive tasks. *Iscience*, 24(10), 2021.

[9] Martin Schrimpf, Idan Asher Blank, Greta Tuckute, Carina Kauf, Eghbal A Hosseini, Nancy Kanwisher, Joshua B Tenenbaum, and Evelina Fedorenko. The neural architecture of language: Integrative modeling converges on predictive processing. *Proceedings of the National Academy of Sciences*, 118(45):e2105646118, 2021.

[10] David Sussillo, Mark M Churchland, Matthew T Kaufman, and Krishna V Shenoy. A neural network that finds a naturalistic solution for the production of muscle activity. *Nature neuroscience*, 18(7):1025–1033, 2015.

[11] Jonathan A Michaels, Stefan Schaffelhofer, Andres Agudelo-Toro, and Hansjörg Scherberger. A goal-driven modular neural network predicts parietofrontal neural dynamics during grasping. *Proceedings of the national academy of sciences*, 117(50):32124–32135, 2020.

[12] Pouya Bashivan, Kohitij Kar, and James J DiCarlo. Neural population control via deep image synthesis. *Science*, 364(6439):eaav9436, 2019.

[13] Pinglei Bao, Liang She, Mason McGill, and Doris Y Tsao. A map of object space in primate inferotemporal cortex. *Nature*, 583(7814):103–108, 2020.

[14] Wolfgang Maass. Networks of spiking neurons: the third generation of neural network models. *Neural networks*, 10(9):1659–1671, 1997.

[15] Chung-Chuan Lo, Leanne Boucher, Martin Paré, Jeffrey D Schall, and Xiao-Jing Wang. Proactive inhibitory control and attractor dynamics in countermanding action: a spiking neural circuit model. *Journal of Neuroscience*, 29(28):9059–9071, 2009.

[16] Kefei Liu, Jingjie Shang, Xiaoxin Cui, Chenglong Zou, Yisong Kuang, Kanglin Xiao, Yi Zhong, and Yuan Wang. How the brain achieves real-time vision: A spiking position perception model. *IEEE Transactions on Cognitive and Developmental Systems*, 2023.

[17] Jindong Liu, David Perez-Gonzalez, Adrian Rees, Harry Erwin, and Stefan Wermter. A biologically inspired spiking neural network model of the auditory midbrain for sound source localisation. *Neurocomputing*, 74(1-3):129–139, 2010.

[18] Alice Geminiani, Claudia Casellato, Alberto Antonietti, Egidio D'Angelo, and Alessandra Pedrocchi. A multiple-plasticity spiking neural network embedded in a closed-loop control system to model cerebellar pathologies. *International journal of neural systems*, 28(05): 1750017, 2018.

[19] Ryan Golden, Jean Erik Delanois, Pavel Sanda, and Maxim Bazhenov. Sleep prevents catastrophic forgetting in spiking neural networks by forming a joint synaptic weight representation. *PLOS Computational Biology*, 18(11):e1010628, 2022.

[20] Xiaolei Zhu, Baixin Zhao, De Ma, and Huajin Tang. An efficient learning algorithm for direct training deep spiking neural networks. *IEEE Transactions on Cognitive and Developmental Systems*, 14(3):847–856, 2021.

[21] Bhaskar Mukhoty, Velibor Bojkovic, William de Vazelhes, Xiaohan Zhao, Giulia De Masi, Huan Xiong, and Bin Gu. Direct training of snn using local zeroth order method. *Advances in Neural Information Processing Systems*, 36:18994–19014, 2023.

[22] Benjamin Cramer, Yannik Stradmann, Johannes Schemmel, and Friedemann Zenke. The heidelberg spiking data sets for the systematic evaluation of spiking neural networks. *IEEE Transactions on Neural Networks and Learning Systems*, 33(7):2744–2757, 2020.

[23] Huijuan Fang, Yongji Wang, and Jiping He. Spiking neural networks for cortical neuronal spike train decoding. *Neural Computation*, 22(4):1060–1085, 2010.

[24] I-A Lungu, Alexa Riehle, Martin P Nawrot, and Michael Schmuker. Predicting voluntary movements from motor cortical activity with neuromorphic hardware. *IBM Journal of Research and Development*, 61(2/3):5–1, 2017.

[25] Fabio Boi, Timoleon Moraitis, Vito De Feo, Francesco Diotalevi, Chiara Bartolozzi, Giacomo Indiveri, and Alessandro Vato. A bidirectional brain-machine interface featuring a neuromorphic hardware decoder. *Frontiers in neuroscience*, 10:563, 2016.

[26] Tengjun Liu, Yansong Chua, Yuxiao Ning, Pengfu Liu, Yiwei Zhang, Tuoru Li, Guihua Wan, Zijun Wan, Weidong Chen, and Shaomin Zhang. motorsrnn: A spiking recurrent neural network inspired by brain topology for the effective and efficient decoding of cortical spike trains. *Biomedical Signal Processing and Control*, 99:106745, 2025.

[27] Guozhang Chen, Franz Scherr, and Wolfgang Maass. A data-based large-scale model for primary visual cortex enables brain-like robust and versatile visual processing. *science advances*, 8(44): eabq7592, 2022.

[28] Nuria Vendrell-Llopis, Ching Fang, Albert J Qü, Rui M Costa, and Jose M Carmena. Diverse operant control of different motor cortex populations during learning. *Current Biology*, 32(7): 1616–1622, 2022.

[29] Emily R Oby, Matthew D Golub, Jay A Hennig, Alan D Degenhart, Elizabeth C Tyler-Kabara, Byron M Yu, Steven M Chase, and Aaron P Batista. New neural activity patterns emerge with long-term learning. *Proceedings of the National Academy of Sciences*, 116(30):15210–15215, 2019.

[30] Darby M Losey, Jay A Hennig, Emily R Oby, Matthew D Golub, Patrick T Sadtler, Kristin M Quick, Stephen I Ryu, Elizabeth C Tyler-Kabara, Aaron P Batista, M Yu Byron, et al. Learning leaves a memory trace in motor cortex. *Current Biology*, 34(7):1519–1531, 2024.

[31] Jay A Hennig, Emily R Oby, Matthew D Golub, Lindsay A Bahureksa, Patrick T Sadtler, Kristin M Quick, Stephen I Ryu, Elizabeth C Tyler-Kabara, Aaron P Batista, Steven M Chase, et al. Learning is shaped by abrupt changes in neural engagement. *Nature Neuroscience*, 24(5): 727–736, 2021.

[32] Matthew D Golub, Patrick T Sadtler, Emily R Oby, Kristin M Quick, Stephen I Ryu, Elizabeth C Tyler-Kabara, Aaron P Batista, Steven M Chase, and Byron M Yu. Learning by neural reassociation. *Nature neuroscience*, 21(4):607–616, 2018.

[33] Apostolos P Georgopoulos, John F Kalaska, Roberto Caminiti, and Joe T Massey. On the relations between the direction of two-dimensional arm movements and cell discharge in primate motor cortex. *Journal of Neuroscience*, 2(11):1527–1537, 1982.

[34] A Bolu Ajiboye, Francis R Willett, Daniel R Young, William D Memberg, Brian A Murphy, Jonathan P Miller, Benjamin L Walter, Jennifer A Sweet, Harry A Hoyen, Michael W Keith, et al. Restoration of reaching and grasping movements through brain-controlled muscle stimulation in a person with tetraplegia: a proof-of-concept demonstration. *The Lancet*, 389(10081): 1821–1830, 2017.

[35] Meel Velliste, Sagi Perel, M Chance Spalding, Andrew S Whitford, and Andrew B Schwartz. Cortical control of a prosthetic arm for self-feeding. *Nature*, 453(7198):1098–1101, 2008.

[36] Dawn M Taylor, Stephen I Helms Tillery, and Andrew B Schwartz. Direct cortical control of 3d neuroprosthetic devices. *science*, 296(5574):1829–1832, 2002.

[37] Qi Zheng, Yiwei Zhang, Zijun Wan, Wasim Q Malik, Weidong Chen, and Shaomin Zhang. Orthogonalizing the activity of two neural units for 2d cursor movement control. In *2020 42nd Annual International Conference of the IEEE Engineering in Medicine & Biology Society (EMBC)*, pages 3046–3049. IEEE, 2020.

[38] Stephen H Scott, Paul L Gribble, Kirsten M Graham, and D William Cabel. Dissociation between hand motion and population vectors from neural activity in motor cortex. *Nature*, 413 (6852):161–165, 2001.

[39] Timothy P Lillicrap and Stephen H Scott. Preference distributions of primary motor cortex neurons reflect control solutions optimized for limb biomechanics. *Neuron*, 77(1):168–179, 2013.

[40] Ed S Lein, Michael J Hawrylycz, Nancy Ao, Mikael Ayres, Amy Bensinger, Amy Bernard, Andrew F Boe, Mark S Boguski, Kevin S Brockway, Emi J Byrnes, et al. Genome-wide atlas of gene expression in the adult mouse brain. *Nature*, 445(7124):168–176, 2007.

[41] Michael J Hawrylycz, Ed S Lein, Angela L Guillozet-Bongaarts, Elaine H Shen, Lydia Ng, Jeremy A Miller, Louie N Van De Lagemaat, Kimberly A Smith, Amanda Ebbert, Zackery L Riley, et al. An anatomically comprehensive atlas of the adult human brain transcriptome. *Nature*, 489(7416):391–399, 2012.

[42] Nicolas Perez-Nieves, Vincent CH Leung, Pier Luigi Dragotti, and Dan FM Goodman. Neural heterogeneity promotes robust learning. *Nature communications*, 12(1):5791, 2021.

[43] Stephen H Scott and John F Kalaska. Reaching movements with similar hand paths but different arm orientations. i. activity of individual cells in motor cortex. *Journal of neurophysiology*, 77 (2):826–852, 1997.

[44] Roger N Lemon. Descending pathways in motor control. *Annu. Rev. Neurosci.*, 31(1):195–218, 2008.

[45] Roger Lemon. Recent advances in our understanding of the primate corticospinal system. *F1000Research*, 8, 2019.

[46] Karunesh Ganguly and Jose M Carmena. Emergence of a stable cortical map for neuroprosthetic control. *PLoS biology*, 7(7):e1000153, 2009.

[47] Jennifer L Collinger, Brian Wodlinger, John E Downey, Wei Wang, Elizabeth C Tyler-Kabara, Douglas J Weber, Angus JC McMorland, Meel Velliste, Michael L Boninger, and Andrew B Schwartz. High-performance neuroprosthetic control by an individual with tetraplegia. *The Lancet*, 381(9866):557–564, 2013.

[48] Roberta M Kelly and Peter L Strick. Cerebellar loops with motor cortex and prefrontal cortex of a nonhuman primate. *Journal of neuroscience*, 23(23):8432–8444, 2003.

[49] Junchol Park, Luke T Coddington, and Joshua T Dudman. Basal ganglia circuits for action specification. *Annual review of neuroscience*, 43(1):485–507, 2020.

[50] María J Cáceres and Ricarda Schneider. Analysis and numerical solver for excitatory-inhibitory networks with delay and refractory periods. *ESAIM: Mathematical Modelling and Numerical Analysis*, 52(5):1733–1761, 2018.

Supplementary material for "Proliferation of cosine-tuning in both artificial spiking and cortical neural networks during learning"

Tengjun Liu[1,2] **Yansong Chua**[3*] **Yiwei Zhang**[1,2] **Yuxiao Ning**[1,2]

Guihua Wan[1] **Zijun Wan**[1,2] **Shaomin Zhang**[1,2,4,5*]

Weidong Chen[1,6]

[1] Key Laboratory of Biomedical Engineering of Ministry of Education, Qiushi Academy for Advanced Studies, Zhejiang University, Hangzhou, China
[2] Department of Biomedical Engineering, Zhejiang University, Hangzhou, China
[3] China Nanhu Academy of Electronics and Information Technology (CNAEIT), Jiaxing, China
[4] State Key Laboratory of Brain-Machine Intelligence, Zhejiang University, Hangzhou, China
[5] the MOE Frontier Science Center for Brain Science & Brain-machine Integration, Zhejiang University, Hangzhou, China
[6] Department of Computer Science and Technology, Zhejiang University, Hangzhou, China
{tengjunliu,zhangevey,ningyuxiao,0916405,11715005,chenwd}@zju.edu.cn
[*]Corresponding authors: shaomin@zju.edu.cn, caiyansong@cnaeit.com

1 Experiments and dataset

1.1 Animal Experiments

Three macaque monkeys (B04, C05, B11) each received a 96-channel microelectrode array (Blackrock Microsystems Inc., USA) implanted in the right primary motor cortex (M1). Monkeys B04 and C05 were trained for joystick control tasks, while C05 and B11 participated in the brain-machine interface (BMI) experiments. All procedures were conducted with approval from the Experimental Animal Welfare Ethics Committee of Zhejiang University.

1.1.1 Experiment Paradigm: joystick control

This study conducted a joystick control experiment to acquire data for training the network model. Monkeys B04 and C05 were trained to use their left hand to operate a joystick while seated in a primate chair, facing a computer screen displaying task instructions. Two circular cursors were shown: a target cursor and a controlled cursor, the latter reflecting the joystick's position. At the start of each trial, the target cursor appeared randomly in one of four directions (*top*, *bottom*, *left*, or *right*), and the monkeys were tasked with aligning the controlled cursor with the target for 300 milliseconds within the 2-second trial duration. Upon successful completion, a reward was given, and a new trial began with a re-randomized target position.

Neural signals and joystick positions were recorded simultaneously using the Cerebus multi-channel data acquisition system (Blackrock Microsystems Inc., USA). Neural activity was sampled at 30 kHz, and joystick data at 1 kHz. Data used in this study was derived from a single session for each monkey.

1^{st} Workshop on NeuroAI @ 38th Conference on Neural Information Processing Systems (NeurIPS 2024).

1.1.2 Experiment Paradigm: BMI

In this study, we conducted the mind control experiments to validate the predictability of the motorSRNN. By assigning different decoders for every experimental section, we could guide the biological neural network in the motor cortex of primates to learn multiple new tasks, thereby obtaining more generalizable results. In this mind control experiment, C05 and B11, seated in a primate chair, were trained to voluntarily modulate their neural activity to complete a 4-radial center-out task. A computer screen in front of the monkeys displayed the operational cues. The collected neural signals were mapped to the movement of the controlled cursor on the screen using a Kalman filter, to align with the target cursor. Other designs were identical to the joystick control experiment. Similarly, during the experiments, the Cerebus multi-channel data acquisition system (Blackrock Microsystems Inc., USA) was utilized to collect the neural signals of the monkeys at a sampling rate of 30 kHz.

Monkeys C05 and B11 were both required to undertake the experiment for 4 sessions. Due to the neural variability [1, 2], the consecutive interval between these sessions was set to around one month, to ensure the composition difference of recorded neuronal groups in different sessions to a large extent for more generalizable results. As shown in Fig. S1, every session consisted of a look block, several assisted mind control blocks and pure mind control blocks, where the number of assisted and pure MC blocks are determined by the willingness of monkeys. The neural signals collected during the look block were used to establish a new Kalman filter decoder. During the assisted mind control blocks, an auxiliary vector was utilized to aid in guiding a controlled cursor toward the target, and the strength of the auxiliary vector gradually decreased. Finally, the auxiliary vector was eliminated during the pure mind control blocks, thus the monkeys were required to solely rely on modulating their neural activity to control the cursor. In every assisted and pure MC block, the decoder was updated based on neural activities in the last block. The look and pure mind control blocks were identified as the before-training and after-training phases, respectively, while the assisted and pure mind control blocks as a whole were regarded as the during-training phase.

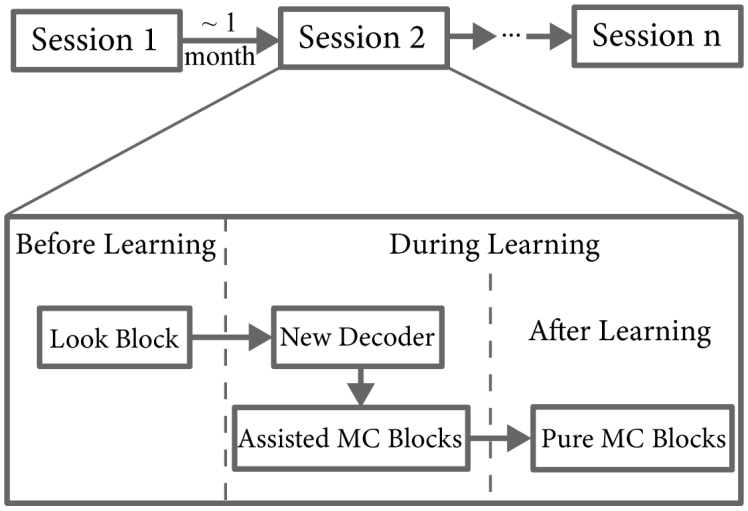

Figure S1: **Timeline of the BMI experiment.** The monkeys completed the mind control experiments for 4 sessions, with consecutive intervals of around 1 month. Every session consisted of a look block, several assisted mind control blocks, and several pure mind control blocks. A new Kalman filter was established by the neural signals collected in the look block. The look and pure mind control blocks were regarded as before training and after training, respectively, while the assisted and pure mind control blocks were considered during training.

1.2 Signal Processing

1.2.1 Joystick control experiment

The raw neural signals were first filtered using a 4th-order Butterworth high-pass filter at 250 Hz to isolate spike trains. Spikes were identified with a detection threshold set at 4.5 times the root mean square (RMS) of the baseline signal. Offline Sorter (Plexon Inc., USA) then classified the

detected spikes into individual neurons based on waveform similarity and principal component distribution. This process yielded 157 and 153 spike trains for B04 and C05, respectively, which were downsampled to 10 kHz for computational efficiency. Joystick position signals were smoothed using a 20-point moving average filter.

To account for neural transmission delays to the muscles, data segmentation incorporated delays of 120 ms for B04 and 140 ms for C05. Neural signals were segmented using a 50 ms time window, and corresponding joystick velocities were adjusted for the delay. Velocity samples that crossed a speed threshold were categorized by direction: *Top* (45° to 135°), *Bottom* (-135° to -45°), *Right* (135° to 225°), and *Left* (-45° to 45°). Post-segmentation, 1981 samples for B04 and 3755 for C05 were obtained. From these, 1/10 of the samples were randomly chosen for validation, with the remaining used for training. Separate datasets were then constructed for B04 and C05.

1.2.2 BMI experiment

Similarly, a 250 Hz 4th-order Butterworth high-pass filtering was first applied to the neural signals. Next, to reduce the influence of the recording instability during the experiments, we set the threshold for spike detection to 8.0 times the RMS of the baseline signal. The spikes were sorted out online based on the waveform shape. Signals of all the first collected neuron in every valid channel were mapped to the movement of the controlled cursor via a Kalman filter. In each trial, we decoded the cursor velocity every 30 ms, then calculated and updated the cursor position on the screen.

2 motorSRNN: an SNN architecture inspired by the motor circuit in primates

spiking recurrent neural networks (SRNNs) have been shown prosiming in many different tasks [3, 4]. The motorSRNN, an spiking neural network (SNN) architecture modeled after primate motor circuits (Fig. S2B), aims to reconstruct the pathway between the brain and the externals. It incorporates distinct layers representing the the motor cortex (MC), subcortical region (SC), spine (Sp) and muscles (Ms) (Fig. S2A). Following principles of modularity [5] and hierarchy [6], the motor cortex is divided into three layers: the input layer, MC1, and MC2. The input layer itself yields the cortical spike trains (CSTs) collected from the M1 of monkeys. Layer MC1 receives these CSTs, while layer MC2, a lower-level module, is not directly connected to the input layer. To introduce modularity, the MC1 and MC2 modules are sparsely connected, where 20% of the connections are randomly set to zero. In the primate motor cortex, certain neurons transmit signals to the subcortical region, while others connect directly to motoneurons via cortico-motoneuronal (CM) pathways, which are specific to primates [7] (Fig. S2B, right dashed rectangle). In motorSRNN, layer SC receives inputs from MC1 and MC2, and sends feedback to them, mimicking the role of the thalamus in biological systems (Fig. S2B, left dashed rectangle). Additionally, layer Ms receives direct inputs from the input layer via a long-loop connection (M1LC), analogous to the biological CM pathway. Layer Sp processes outputs from the basal ganglia in SC and sends signals to Ms. SRNNs are implemented in MC1, MC2, and SC [8, 9], while a feedforward SNN operates in layer Sp. For enhanced biological realism, distance-dependent connectivity is applied, where connection strength diminishes with increasing distance [10]. Finally, layer Ms outputs cumulative probabilities for four movement directions (*up*, *down*, *left*, *right*) in a 50 ms time window. The predicted direction is determined by the maximum cumulative probability at the final moment.

2.1 Neuron Models

2.1.1 Firing-threshold ALIF neurons

ALIF neurons build up the SNN in layer MC 1, MC 2, SC, and Sp in the motorSRNN, for its better biological plausibility [12] and performance in classification [13] than traditional leaky integrate-and-fire (LIF) models. An ALIF neuron receives the spikes emitted by the presynaptic input ALIF neurons. The received spikes cause the ALIF neurons' membrane potential to increase. When an ALIF neuron's membrane potential reaches the firing threshold, it emits a spike. And then its membrane potential will be reset to the resting potential (set to 0 in this study), and its firing threshold will increase. When no spike is received, the membrane potential and firing threshold of the ALIF neuron will both gradually decrease.

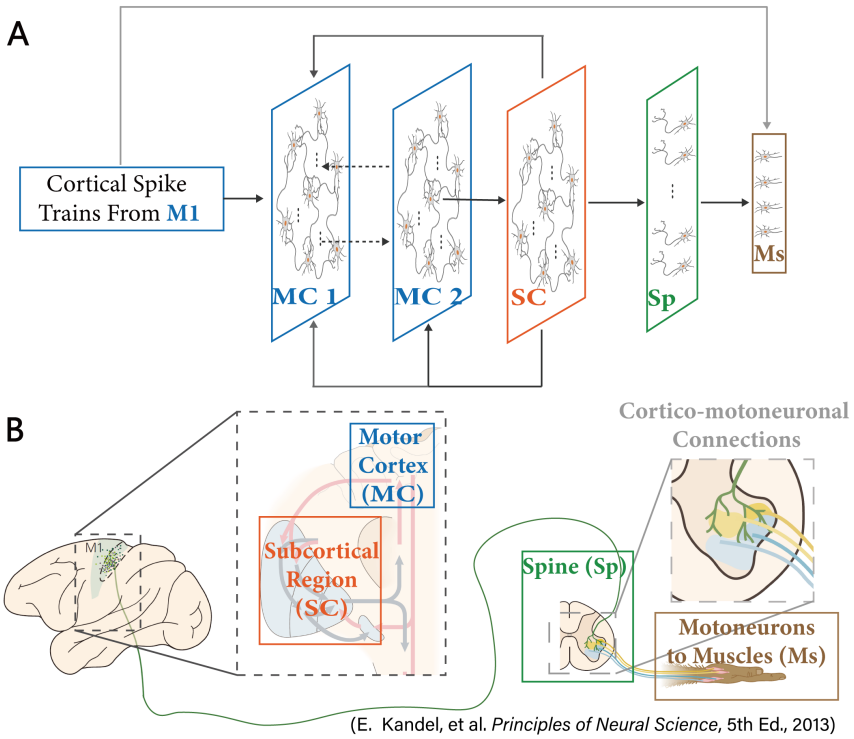

Figure S2: **Architecture of motorSRNN.** (A) The architecture of motorSRNN. Different layers represent different structures solidly framed in corresponding colors in (B). The SNNs in MC1, MC2, and SC are recurrent, while the one in Sp is feedforward. The neurons in layer MC1, MC2, SC, Sp are ALIF models, and the ones in layer Ms are LI models. MC1: motor cortex module 1, MC2: motor cortex module 2, SC: subcortical region, Sp: spine. Solid arrows denote full connections, and dashed arrows indicate sparse initialized connections. The darker the arrow, the stronger the initialized connection is. (B) The motor circuit in primates, modified from [11].

Eq. (1) describes the dynamical process of an ALIF neuron's membrane potential.

$$u_t = \alpha u_{t-1} + (1-\alpha) R_m I_t - s_{t-1}\theta \tag{1}$$

where u_t denotes the membrane potential at time t, u_{t-1} denotes the membrane potential at time $t-1$; α represents the decay coefficient of the membrane potential, as shown in Eq. (2); R_m indicates the constant membrane resistance of the ALIF neuron; I_t is the total current received from the presynaptic ALIF neurons, as shown in Eq. (3); s_{t-1} denotes the spiking state of an ALIF neuron at time $t-1$, as shown in Eq. (4); and θ indicates the dynamical firing threshold, as shown in Eq. (5).

$$\alpha = \exp\left(-\frac{dt}{\tau_m}\right) \tag{2}$$

where dt denotes the unit time, τ_m represents the time constant (TC) of the membrane potential.

$$I_t = \sum_i s_t \tag{3}$$

where i indicates the index of the presynaptic ALIF neurons connected to the current ALIF neuron, and s_t denotes the spiking state of the connected ALIF neuron at time t. That is, Eq. (3) shows that the input current of an ALIF neuron at the current moment is the sum of the number of spikes from the presynaptic ALIF neurons at the current moment.

$$s_t = \begin{cases} 1, & u_t \geq \theta \\ 0, & u_t < \theta \end{cases} \tag{4}$$

When s_t equals 1, it means that the ALIF neuron fires at time t, while when s_t equals 0, it means there is no spike fired at time t.

$$\theta = b_0 + \beta\eta_t \tag{5}$$

where b_0 indicates the minimal firing threshold, and the product of β and η_t denotes the change of the dynamical threshold θ at time t, within which β is a constant, and η_t is calculated as shown in Eq. (6).

$$\eta_t = \rho\eta_{t-1} + (1-\rho)s_{t-1} \tag{6}$$

where ρ represents the decay coefficient of the dynamical firing threshold, as shown in Eq. (7).

$$\rho = \exp\left(-\frac{dt}{\tau_{adp}}\right) \tag{7}$$

where τ_{adp} denotes the TC for the decay of the dynamical firing threshold.

2.1.2 Non-firing a LI neurons

LI neurons are used to mimic the continuity of muscles in layer Ms of the motorSRNN. LI neurons receive spikes from presynaptic ALIF neurons. The received spikes will cause the membrane potential of the current LI neurons to increase, but unlike ALIF neurons, LI neurons will only accumulate membrane potentials, but not fire. Similarly, when no spike is received, the membrane potential of the current LI neuron will gradually decrease. The membrane potential u_t^{LI} is updated as shown in Eq. (8).

$$u_t^{LI} = \alpha^{LI} u_{t-1}^{LI} + (1-\alpha^{LI}) R_m^{LI} I_t^{LI} \tag{8}$$

where the other relative variables and their updating equations are the same as those of ALIF neurons.

2.2 Training

In SNNs, surrogate gradients provide a smooth, differentiable approximation of the true gradient, enabling backpropagation in networks with non-differentiable spiking neurons. This approach allows efficient training using standard gradient-based optimization methods [14]. In the motorSRNN, surrogate gradients are computed, and the trainable parameters—including feedforward and recurrent weights, membrane TC τ_m, and adaptive threshold TC τ_{adp}—are updated using backpropagation-through-time and the Adam optimizer. Feedback connections remain fixed after initialization.

Key parameter settings refer to Tab. S1. The size of the input layer equals the amount of the collected biological neurons. The output layer contains 4 LI neurons corresponding to 4 labels. The LI neuron with the highest membrane potential indicates the output at every time step. A softmax function is utilized to convert the membrane potential to the probability. The accumulated probabilities of 4 output neurons over all time steps are the final output of the network. The largest accumulated probability denotes the output label. All the models are implemented with PyTorch 1.8.1 and trained on two NVIDIA GeForce RTX 3090.

3 Cosine-tuning Analysis

3.1 Cosine-tuning neurons in the motor cortex

In 1982, the firing rates of many pyramidal neurons in the M1 of monkeys were found to vary systematically with the direction of monkeys' hand movements [15]. A neuron exhibited the highest firing rate when a monkey moved its hand to the neuron's preferred direction (PD), and the firing rate decreased as movements deviated from the PD. This relation between the firing rate (F) of a specific neuron and the direction of movements of the monkeys' hands (δ) could be fitted by a cosine function as shown in Eq. 9:

$$F = f_0 + g\cos(\delta - \delta_0) \tag{9}$$

where f_0 denotes the baseline firing rate, g indicates the modulation depth, and δ_0 represents the PD.

Table S1: **Key parameter settings of the motorSRNN for both datasets.** τ_{mh} and τ_{adph} denote the membrane and adaptive TCs in the hidden layers. τ_{mo} indicates the membrane TCs in the output layer. R_m & R_m^{LI}, β, and b_0 are parameters describing the neuronal dynamics represented in the equations.

Dataset	B04	C05
Hidden Layers Size	[64, 32, 16, 8]	[64, 32, 16, 8]
τ_{mh}	1	1
τ_{adph}	5	5
τ_{mo}	1.5	1.5
R_m & R_m^{LI}	1.4	1.4
β	1.8	1.8
b_0	0.01	0.01
Batch Size	32	32
Loss Function	Cross-entropy	Cross-entropy
Epochs	30	30
Learning Rate (LR)	1e-2	8.75e-3
LR Decay Type	Step	Step
LR Decay	0.7 per 20 epochs	0.5 per 20 epochs

3.2 Resultant vector length and the distributional symmetry

Symmetry has been found to be an important feature of the neuronal PD distributions in the motor cortex of primates [16–18]. In circular statistics, the distributional symmetry of data points on the unit circle can be deduced by the resultant vector length (RVL). Every data point r_j represents an angle γ_j, as shown in Eq. 10:

$$\mathbf{r}_j = \begin{pmatrix} \cos\gamma_j \\ \sin\gamma_j \end{pmatrix} \tag{10}$$

where j indicates the index of the data point. Next, RVL is the length of the average vector of all the data points, as shown in Eq. 11:

$$\mathrm{RVL} = \left\| \frac{1}{N_s} \sum_j \mathbf{r}_j \right\|, \tag{11}$$

where N_s denotes the total number of data points. The closer the RVL is to 0, the more symmetrical the distribution of data points is. On the contrary, if the RVL equals 1, the data points totally concentrate in one single direction. In this study, every data point on the unit circle means the PD of an significantly cosine-tuned neuron (SCtN). That is, a smaller RVL indicates a more symmetrical distribution of the PDs of the SCtNs. Note that the symmetry is defined on polar coordinate, thus an absolute symmetry satisfies $N_\gamma = N_{\gamma+\pi}$, where $N_{\gamma+\pi}$ and N_γ represent the numbers of data points with certain angles γ and $\gamma + \pi$, respectively. CircStats, an MATLAB toolbox, was employed for the aforementioned calculation [19].

4 Statistical Analysis

F-test was applied to determine whether the cosine fitting regression is significant. $p < 0.05$ indicates a significant dependency between the response and predictor variables. In the motorSRNN, since there are four predictor variables and three parameters to be fitted in the cosine function, only the fitting with very high R^2 can pass the statistical test.

The significance of distributional differences was judged by a 2-sample t-test. The null hypothesis is that the two groups of data to be tested are independent random samples from normal distributions with equal means. $p < 0.05$ indicates a significant distributional difference. Smaller p-value indicates stronger significance.

5 Supplementary results

Here we provided additional example SCtNs in layer MC1 of motorSRNN, as shown in FIg. S3.

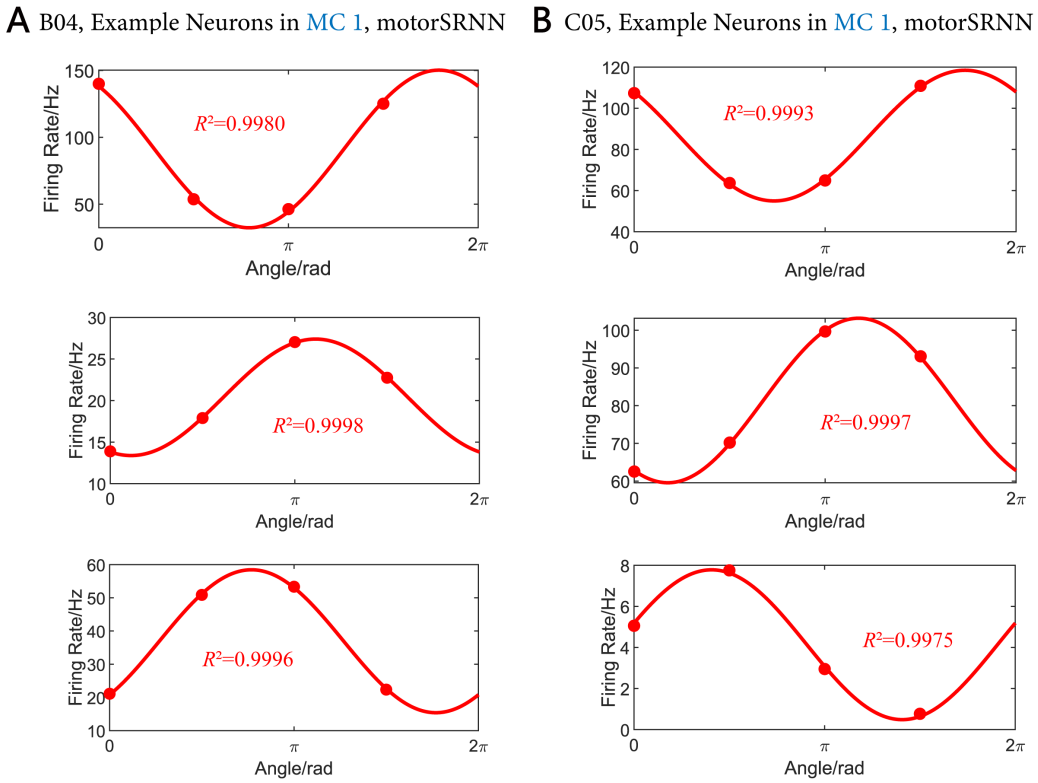

Figure S3: **Example significant cosine-tuning neurons (SCtNs) in the MC1, motorSRNN trained on both the datasets of B04 and C05.** Note that angles are circular, i.e., $f(x) = f(x + 2\pi)$. A unimodal or a monotonic function can not fit the data well.

6 Supplementary discussion

6.1 Implications for neuroscience

After training the motorSRNN, a topologically brain-inspired SNN, we discovered several bio-functional similarities at single-neuron, population, and circuit levels. Firstly, at the single-neuron level, the neurons in the motor cortex, corresponding to layer MC1 of motorSRNN, possess an essential characteristic of cosine-tuning [15]. And we found that more cosine-tuned neurons emerged in layer MC1 of motorSRNN, besides those induced by the input. Secondly, at the population level, a symmetrical distribution of PDs of SCtNs in layer MC1 of motorSRNN was observed, in line with reports in the literature [16–18]. Thirdly, at the circuit level, previous studies have established that the biological CM connections, the counterpart of M1LC, primarily contribute to the dexterous control of hands and fingers [20]. Similarly, after ablating M1LC, the standard deviations of decoding performance over 10 random initialization at each epoch significantly increased. As far as the authors are aware, these bio-functional similarities were observed for the first time in a goal-driven SNN model.

Due to these discoveries of bio-functional similarities, we hypothesize that the motorSRNN can provide valuable insights into the biological motor circuit. Based on the proliferation and persistency of cosine-tuning observed in layer MC1 of motorSRNN, we predict that new task learning can also induce such proliferation and persistency in the biological motor cortex. To validate this prediction, we designed a BMI experiment, where monkeys need to learn to modulate the activities in their cortical neural networks to adapt to a new Kalman filter decoder. And the results confirmed that new

task learning indeed induces both the proliferation and persistency of cosine-tuning in the primate motor cortex.

Task-tuning should definitely appear in decoding, however, it is not necessarily cosine-like. In our study, the analysis of cosine-tuning was based on a statistical F-test for fitting. Thus, only neurons passing the test would be further considered. In a classical work, Perge et al. also fitted neuronal firing rates with four directions using a cosine function, based on statistical F-tests [21]. But importantly, we emphasize that the purpose of our cosine-tuning investigation is to establish the biological consistency of the proposed motorSRNN and the biological motor circuit, rather than to exclude other possible mathematical fitting functions.

In this study, we focused on training motorSRNN for classification instead of regression as an initial step to validate the feasibility of applications of SNN on invasive BMI. However, it should not be inferred that the role of the motor cortex is just for classification. The motor cortex's primary function is to generate motion, which is a complex process that cannot be simply reduced to a classifier or regressor. Nevertheless, classification, in our view, represents a reasonable simplification, which can still facilitate our understanding of neural systems to some degree. Notably, the continuity of muscles was also considered in the motorSRNN, so that the output neurons were non-spiking integrators. The classification targets could be regarded as the directions of "muscles" in the output layer. Even under such simplification, some bio-functional similarities still emerged in the proposed motorSRNN. Similarly, although the convolutional neural network, a classifier, have been widely accepted as neural models of the visual system by the community [22–25], we cannot assert that the visual cortex solely performs image classification.

6.2 Comparison between motorSRNN and other goal-driven DL models

Bio-functional similarities and predictability of neural computations Bio-functional similarities have been reported in numerous goal-driven DL models at different levels, as shown by the following examples. At the single-neuron level, Khaled et al. found that ANNs can spontaneously develop numerosity-selective neurons similar to those found in the biological brain [26]. At the population level, Katharina et al. showed that ANNs can exhibit functional separations for objects and faces, just like the biological brain [23]. At the circuit level, Shahab et al. demonstrated that self-supervision can promote the emergence of both the biological ventral and dorsal pathways in a deep neural network [25]. Moreover, David et al. found that artificial neurons in a recurrent neural network (RNN) can closely resemble the dynamics of motor cortex neurons in monkeys at both the single-neuron and population levels [27]. In our study, the motorSRNN showed the bio-functional similarities at all single-neuron, population, and circuit levels. These bio-functional similarities have motivated researchers to seek potential neuroscientific inspirations from ANNs. For example, Pouya et al. developed an ANN-driven image synthesis method for predicting neuronal tuning by taking ANNs as models of the primate brain's ventral visual stream [28]. Bao et al. found a hierarchical map of object space in the IT cortex, and further validated it in biology [29]. Inspired by the observation in layer MC1 of motorSRNN in this study, we also validated that training can indeed promote cultivation and persistency of cosine-tuning in the biological motor cortex in primates. Additionally, ablation studies predicted that long-term stable feedback synapses may contribute to the training-induced cultivation of cosine-tuning.

6.3 Goal-driven SNN models for neural computation

Importantly, the significance of this work goes beyond the proposition of motorSRNN, as it introduces a novel framework for building models of neural computation. Incorporating biological signals as input enhances the authenticity of models and potentially results in more biologically plausible representations. Consequently, such models are likely to exhibit more bio-functional similarities and offer valuable insights into the mechanisms of neural computation. The proposed motorSRNN demonstrated bio-functional similarities at the single-neuron, population, and circuit levels, and generated the prediction of the presence of learning-induced proliferation and persistency of cosine-tuning in the biological motor cortex, which we also validated by BMI experiments in monkeys. However, the utilization of this framework should be approached with caution. The bio-functional similarities directly arising from biological signal input must be accounted first, before identifying emergent bio-functional similarities. In this study, the occurrence of cosine-tuning before training was not surprising, but the emergence of more cosine-tuned neurons after training was a novel finding.

References

[1] David Sussillo, Sergey D Stavisky, Jonathan C Kao, Stephen I Ryu, and Krishna V Shenoy. Making brain–machine interfaces robust to future neural variability. *Nature communications*, 7 (1):13749, 2016.

[2] John E Downey, Nathaniel Schwed, Steven M Chase, Andrew B Schwartz, and Jennifer L Collinger. Intracortical recording stability in human brain–computer interface users. *Journal of neural engineering*, 15(4):046016, 2018.

[3] Bojian Yin, Federico Corradi, and Sander M Bohté. Effective and efficient computation with multiple-timescale spiking recurrent neural networks. In *International Conference on Neuromorphic Systems 2020*, pages 1–8, 2020.

[4] Bojian Yin, Federico Corradi, and Sander M Bohté. Accurate and efficient time-domain classification with adaptive spiking recurrent neural networks. *Nature Machine Intelligence*, 3 (10):905–913, 2021.

[5] Asaf Keller. Intrinsic synaptic organization of the motor cortex. *Cerebral Cortex*, 3(5):430–441, 1993.

[6] Robert J Morecraft and Gary W van Hoesen. Frontal granular cortex input to the cingulate (m3), supplementary (m2) and primary (m1) motor cortices in the rhesus monkey. *Journal of Comparative Neurology*, 337(4):669–689, 1993.

[7] Roger N Lemon. Descending pathways in motor control. *Annu. Rev. Neurosci.*, 31(1):195–218, 2008.

[8] Charles Capaday, Christian Ethier, Laurent Brizzi, Attila Sik, Carl van Vreeswijk, and Denis Gingras. On the nature of the intrinsic connectivity of the cat motor cortex: evidence for a recurrent neural network topology. *Journal of neurophysiology*, 102(4):2131–2141, 2009.

[9] David G Beiser, Sherwin E Hua, and James C Houk. Network models of the basal ganglia. *Current opinion in neurobiology*, 7(2):185–190, 1997.

[10] Yuru Song, Douglas Zhou, and Songting Li. Maximum entropy principle underlies wiring length distribution in brain networks. *Cerebral cortex*, 31(10):4628–4641, 2021.

[11] Eric R. Kandel, James H. Schwartz, Thomas M. Jessell, Steven A. Siegelbaum, and A. Hudspeth. *Principles of Neural Science*. McGraw-Hill Education, New York, fifth edition edition, 2013. McGraw-Hill's AccessMedicine.

[12] Alexander Rauch, Giancarlo La Camera, Hans-Rudolf Luscher, Walter Senn, and Stefano Fusi. Neocortical pyramidal cells respond as integrate-and-fire neurons to in vivo–like input currents. *Journal of neurophysiology*, 90(3):1598–1612, 2003.

[13] Guillaume Bellec, Darjan Salaj, Anand Subramoney, Robert Legenstein, and Wolfgang Maass. Long short-term memory and learning-to-learn in networks of spiking neurons. *Advances in neural information processing systems*, 31, 2018.

[14] Emre O Neftci, Hesham Mostafa, and Friedemann Zenke. Surrogate gradient learning in spiking neural networks: Bringing the power of gradient-based optimization to spiking neural networks. *IEEE Signal Processing Magazine*, 36(6):51–63, 2019.

[15] Apostolos P Georgopoulos, John F Kalaska, Roberto Caminiti, and Joe T Massey. On the relations between the direction of two-dimensional arm movements and cell discharge in primate motor cortex. *Journal of Neuroscience*, 2(11):1527–1537, 1982.

[16] Stephen H Scott and John F Kalaska. Reaching movements with similar hand paths but different arm orientations. i. activity of individual cells in motor cortex. *Journal of neurophysiology*, 77 (2):826–852, 1997.

[17] Stephen H Scott, Paul L Gribble, Kirsten M Graham, and D William Cabel. Dissociation between hand motion and population vectors from neural activity in motor cortex. *Nature*, 413 (6852):161–165, 2001.

[18] Timothy P Lillicrap and Stephen H Scott. Preference distributions of primary motor cortex neurons reflect control solutions optimized for limb biomechanics. *Neuron*, 77(1):168–179, 2013.

[19] Philipp Berens. Circstat: a matlab toolbox for circular statistics. *Journal of statistical software*, 31:1–21, 2009.

[20] Roger Lemon. Recent advances in our understanding of the primate corticospinal system. *F1000Research*, 8, 2019.

[21] János A Perge, Shaomin Zhang, Wasim Q Malik, Mark L Homer, Sydney Cash, Gerhard Friehs, Emad N Eskandar, John P Donoghue, and Leigh R Hochberg. Reliability of directional information in unsorted spikes and local field potentials recorded in human motor cortex. *Journal of neural engineering*, 11(4):046007, 2014.

[22] Daniel LK Yamins and James J DiCarlo. Using goal-driven deep learning models to understand sensory cortex. *Nature neuroscience*, 19(3):356–365, 2016.

[23] Katharina Dobs, Julio Martinez, Alexander JE Kell, and Nancy Kanwisher. Brain-like functional specialization emerges spontaneously in deep neural networks. *Science advances*, 8(11): eabl8913, 2022.

[24] Seyed-Mahdi Khaligh-Razavi and Nikolaus Kriegeskorte. Deep supervised, but not unsupervised, models may explain it cortical representation. *PLoS computational biology*, 10(11): e1003915, 2014.

[25] Shahab Bakhtiari, Patrick Mineault, Timothy Lillicrap, Christopher Pack, and Blake Richards. The functional specialization of visual cortex emerges from training parallel pathways with self-supervised predictive learning. *Advances in Neural Information Processing Systems*, 34: 25164–25178, 2021.

[26] Khaled Nasr, Pooja Viswanathan, and Andreas Nieder. Number detectors spontaneously emerge in a deep neural network designed for visual object recognition. *Science advances*, 5(5): eaav7903, 2019.

[27] David Sussillo, Mark M Churchland, Matthew T Kaufman, and Krishna V Shenoy. A neural network that finds a naturalistic solution for the production of muscle activity. *Nature neuroscience*, 18(7):1025–1033, 2015.

[28] Pouya Bashivan, Kohitij Kar, and James J DiCarlo. Neural population control via deep image synthesis. *Science*, 364(6439):eaav9436, 2019.

[29] Pinglei Bao, Liang She, Mason McGill, and Doris Y Tsao. A map of object space in primate inferotemporal cortex. *Nature*, 583(7814):103–108, 2020.